# OPERATING CHARACTERISTICS OF A HIGH CURRENT ELECTROSTATIC ACCELERATOR FOR A CONTRABAND DETECTION SYSTEM

S.T. Melnychuk, E. Kamykowski, J. Sredniawski, T. Debiak, AES Inc., Medford NY; R. Ruegg, B. Milton, TRIUMF


*Abstract*

We will describe the operation of a tandem accelerator based Contraband Detection System (CDS) built jointly by Advanced Energy Systems (AES) and TRIUMF, which employs the Nuclear Resonance Absorption (NRA) technique for detecting the attenuation of 9.17 MeV gamma rays by $^{14}$N. A key technology of the CDS device is a high current tandem accelerator designed to provide a 1.76 MeV, 10 mA proton beam to a high power thin film $^{13}$C target. We will describe the operation of the accelerator and present data on the measured output current, emittance, and energy spread using the integrated $^{13}$C target yield. This system has been used to generate images of explosive simulants which can be separated from non-nitrogenous background.


*This work was conducted under FAA. contract # DTFA03-97-D-00012*

## 1 INTRODUCTION

The potential of GRA for detection of explosives has been cited in previous work [1,2]. Development of a high-current electrostatic accelerator for the Contraband Detection System (CDS) uses state-of-the-art technology that is beneficial to other applications like radiography or medical therapies. In this paper we will present some of the data on the current transmission of the accelerator, the radiation field around the machine during operation , measurements of the output beam emittance and energy spread, and show an example of an image generated by the CDS system.

## 2 ACCELERATOR DESIGN

The CDS accelerator system schematic is shown in fig, 1. The system consists of an H- injector and LEBT, the tandem accelerator, an HEBT section with a dipole bend magnet, a $^{13}$C target, a diagnostic vessel and beam dump, and a gamma ray detection and imaging system.

The ion injector uses a filament driven volume H- source with a 2 grid extraction system. Beam is matched to the tandem with a single solenoid magnet. A beam collimator consisting of four independent jaws is used to scrape beam halo and to limit the tandem input current while operating the ion source and extractor in “off-perveance” mode. A fast beam kicker dipole magnet is located after the LEBT solenoid in order to kick the tandem input beam into a water cooled beam stop in the event of an interlock trip generated either by a safety system, or the tandem sub-system.

The HEBT consists of 4 independently adjustable quadrupole magnets (aperture radius: 2.1 cm, pole tip length: 10 cm, gradient: 0.892 T/m/Amp) positioned in pairs on either side of a dipole magnet designed to bend the beam 80.66 deg onto the gamma production target, and several sets of adjustable collimators. The tandem output beam is transported either to a diagnostic station and beam dump or to the gamma production target. The HEBT is capable of producing a variety of elliptical beam spots on target.

The target consists of a $^{13}$C thin film sputtered onto a Ta foil mounted onto a water cooled Cu structure. The target is designed to accommodate the full 17.6 kW beam load. Details of the target design are given in [3,4].

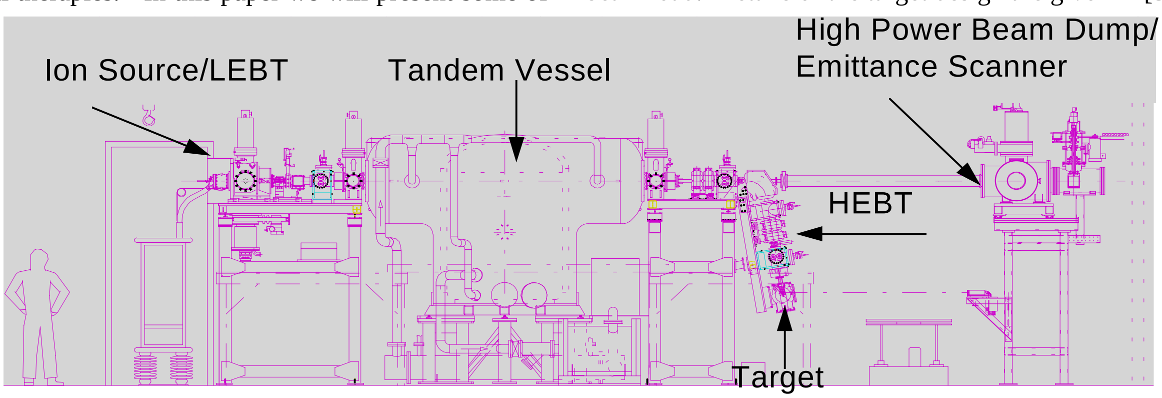


Figure 1. CDS Beamline.

The optical system was designed for matching a 40 kV, 10 mA H- beam to the tandem acceptance. End to end particle simulations of the beamline have been conducted [5] and show that almost no beam loss is expected despite significant space charge induced non-linearity. The physical apertures in the system are designed to be six times the rms radius of the matched beam.

Details of the tandem accelerator design have been presented in [6]. Figure 2 shows some of the accelerator details. The key features of the design consist of a compact power supply designed for 20 mA and 1MV

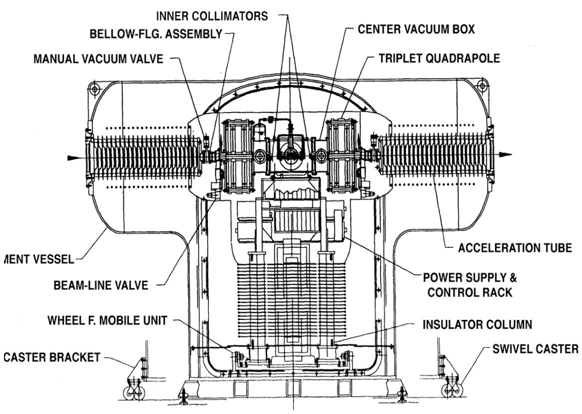


Figure 2. Tandem Accelerator Details.

output voltage, 2 acceleration tubes with a 10 cm aperture designed for 50 kV/inch acceleration gradient, a terminal housing a vapor stripper cell, cryo cold heads, a pair of triplet magnets for matching to the stripper, and all associated power supplies. The terminal equipment is fed by a 4 kW, 1:1 isolation transformer. The SF6 gas is used as the coolant for all the equipment by passing the gas through a heat exchanger. The accelerator vessel was designed conservatively so as not to exceed 177 kV/mm operating at 865 kV terminal voltage and 60 psig of SF6. To date we have not experienced any obvious breakdowns to the vessel walls from the terminal.

Initial tandem commissioning focussed on high voltage related troubleshooting issues. The HV power supply has proven to be very robust in terms of voltage holding capability and survivability of components during HV breakdowns. This power supply was tested at TRIUMF to 1 MV and 26 kW into a water load at 60 psig of SF6. Commissioning of the integrated structure shown in fig. 2 focussed on optimizing the voltage standoff and protection of power supplies in the terminal during HV sparks. This later issue was addressed by Faraday shielding wherever possible, use of low inductance ground straps to tie all terminal power supply cases to the terminal potential, and use of filters on all data, output and power lines for the power supplies. High voltage standoff development focussed on proper configuration of insulators spanning the gap from terminal voltage to ground.

All breakdown problems experienced during commissioning have been due to surface breakdowns along ungraded insulators. In order to inhibit the surface breakdowns it was necessary to electrically segment the insulators spanning the full terminal voltage, and tie the subsections to the high voltage power supply stack at equally spaced intervals to maintain a fixed gradient.

The grading scheme used has virtually eliminated the insulator breakdowns experienced early in the commissioning phase. Initial voltage conditioning after handling components generally takes 1 to 4 hours. Subsequently the terminal can be ramped to operating voltage within a few minutes.

## 3 BEAM OPERATION

The accelerator has been operated with beam at terminal voltages from 600 to 900 kV. Fig. 3 shows the input and output current as a function of the ion source grid 1 voltage. The present experiments are geared toward optimizing the beam tune to minimize beam loss in the terminal, and minimize the radiation field at the operator station located approx. 5 m from the accelerator.

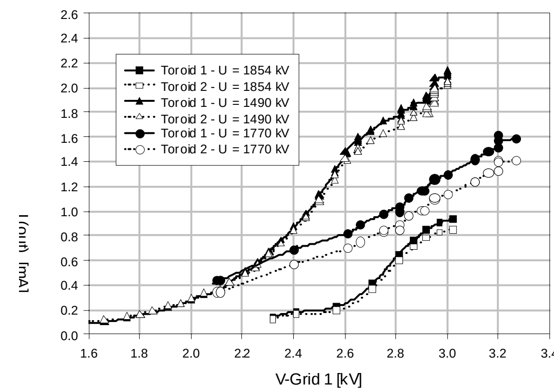


Figure 3. Tandem input and output current vs. Ion source grid 1 voltage at various beam energies. Solid : input; Open: output.

The highest beam current transported through the accelerator to the beam dump is approximately 2.2 mA at 775 kV terminal voltage. The transmission is optimized by variation of the tandem input beam parameters primarily via ion source arc current adjustment, ion source grid 1 voltage, LEBT collimator aperture setting, and via adjustment of the upstream terminal quadrupole triplet used for matching the beam to the stripper channel. Tandem output current measured with a DC beam toroid, and beam scrape-off measured as a temperature rise on a four quadrant collimator diagnostics located in the terminal provide the primary beam tune feedback.

Measurements of the x-rays generated from the tandem during beam operation at 775 kV terminal voltage show that the spectrum is peaked at 135 kV, and the shape is largely independent of the beam, i.e. we get roughly the same spectrum with beam on or beam off. Dose measurements at the containment vessel surface show a linear increase as a function of the input beam current with the dose at the tandem input side being 6 to 10 times greater than at the tandem exit. At 1.5 mA input current the contact dose at the tandem entrance is approximately 300 mR/hr, while the dose at the tandem exit is 40 mR/hr. This shows that the majority of radiation is produced in the H- column which does not have magnetic electron /x-ray suppression.

Measurements of the beam emittance in the horiz.

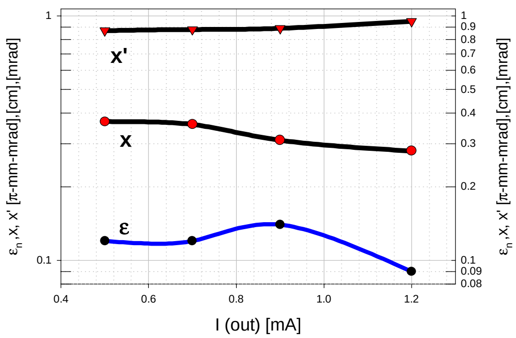


Figure 4. Tandem output beam emittance, divergence and beam size vs. Output current.

plane show that the normalized rms emittance is 0.09 π-mm-mrad at 1.2 mA with an rms beam size of 2.9 mm, and a .94 mrad rms divergence. In the present configuration measurements in the bend plane of the magnet are not available. These data were taken with the emittance scanner located in the diagnostic station as shown in figure 1. The drift distance from the scanner to the center of the downstream quadrupole is 375.6 cm with quads set to 4.5 T/m.

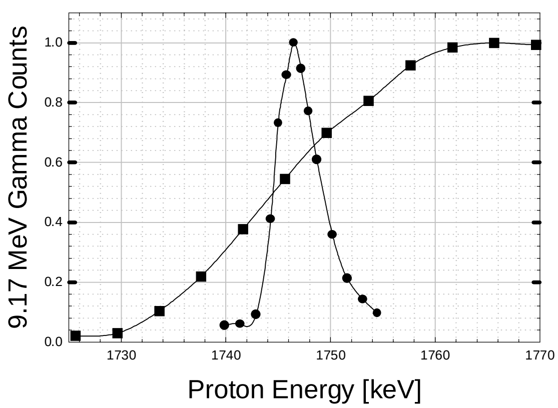


Figure 5. 9.17 MeV gamma ray yield vs. Proton energy. (■) CDS accelerator 2 μm target. (•) VandeGraff, 0.25 μm target.

Figure 5 shows the yield curve for 9.17 MeV gamma rays obtained from a 2μm thick $^{13}$C target measured on the CDS system compared with yield measurements from a 0.25 μm $^{13}$C target done on a Van de Graff system .

The comparison of the two curves show that the thin target yield peak occurs at 1.746 MeV as expected and corresponds with the half maximum point of the 2μm target yield from the CDS accelerator. The 2μm thick target is sufficiently thick to generate gamma rays through the entire CDS beam energy spread and shows that energy is properly calibrated and gives a FWHM CDS energy spread of 15 keV. This is well within the requirements for the CDS system.

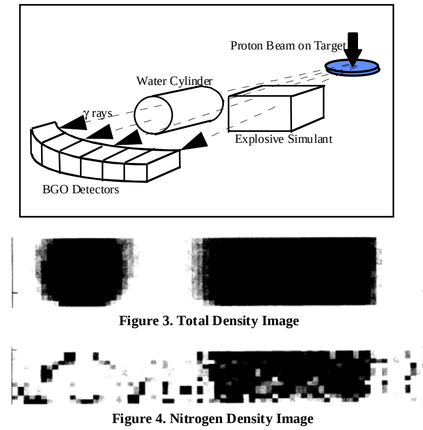


Figure 6. Gamma ray image showing discrimination of nitrogenous explosive simulant from equal density non-nitrogenous phantom.

Using the gamma rays generated by this system we performed a basic imaging experiment designed to demonstrate the ability of the CDS system to discriminate nitrgenous and non-nitrogenous materials of equal density. . Figure 6 shows the gamma ray image obtained with an array of 7 segmented BGO detectors. The items imaged consisted of a cylinder of water and a volume of melamine used as an explosive simulant. The beam current on target was approximately 200 μA. Data was collected by first imaging the water cylinder and melamine in the resonant position, followed by displacing the detector array and phantoms out of the resonant cone and repeating the scan in the non-resonant position. The upper image in fig. 6 shows the non-resonant image proportional to total line density, and the lower image shows the nitrogen density image obtained by subtracting the resonant and non-resonant images. We can see that only the nitrogenous phantom remains visible.

## 4 REFERENCES

1. Gozani, T., "Nuclear Based Techniques for Cargo Inspection - A Review", *Proceedings of Contraband and Cargo Inspection Technology International Symposium*, pp. 9-19, October, 1992.
2. Vartsky, D., et al., "A Method for Detection of Explosives Based on Nuclear Resonance Absorption of Gamma Rays in 14N", *Nuclear Instruments & Methods in Physics Research, Section A 348*, pp. 688-691, 1994.
3. Melnychuk, S.T." Dev. Of a Thin Film 9.17 MeV Gamma Ray Production Target for the CDS". This Conf.
4. Rathke, J. R.,"Engineering Design of a Continuous Duty Gamma Production target for the CDS" This Conf.
5. Reusch, M. F. and Bruhwiler, D. Proc. Of the 18th Int. Linear Accel. Conf., 26-30 Aug. 1996, Geneva, Switz., v.1, p. 358.
6. Milton, B. F., "A High Current Tandem Accelerator for Gamma-Resonance Contraband Detection" 1997 Particle Accelerator Conference, Vancouver CA.